Non-iterative blind data restoration using an extracted filter function

J.N. Caron
Research Support Instruments,
4325-B Forbes Boulevard, Lanham, MD, 20901 USA, caron@researchsupport.com
N.M. Namazi
Electrical Engineering Department, Catholic University of America,
201 Pangborn Hall, Washington, DC 20064, USA
C.J. Rollins
Research Support Instruments,
4325-B Forbes Boulevard, Lanham, MD, 20901 USA

August 30, 2002

Abstract

A signal processing algorithm has been developed where a filter function is extracted from degraded data through mathematical operations. The filter function can then be used to restore much of the degraded content of the data through use of a deconvolution algorithm. This process can be performed without prior knowledge of the detection system, a technique known as blind deconvolution. The extraction process, designated Self-deconvolving Data Reconstruction Algorithm (SeDDaRA), has been used successfully to restore digitized photographs, digitized acoustic waveforms, and other forms of data. The process is non-iterative, computationally efficient, and requires little user input. Implementation is straight-forward, allowing inclusion into many types of signal processing software and hardware.

The novelty of the invention is the application of a power law and smoothing function to the degraded data in frequency space. Two methods for determining the value of the power law are discussed. The first method assumes the power law is frequency-dependent. The function derived comparing the frequency spectrum of the degraded data to the spectrum of a signal with the desired frequency response. The second method assumes this function is a constant of frequency. This approach requires little knowledge of the original data or the degradation.

ocis[100.1830, 100.3020, 100.2000]

1 Introduction

A blind deconvolution technique has been developed that enables efficient restoration and enhancement of degraded data. The process compares the magnitude of the data in Fourier space to the same quality of a specified truth image. A filter function is derived from the comparison and used as a transfer function for restoring the original data. The process, designated self-deconvolving data reconstruction algorithm or SeDDaRA,[1,2] has been successfully applied to digitized images, ultrasound waveforms, and sound recordings. Application requires little user input and is computer efficient.

Signal reconstruction based on deconvolution has been thoroughly studied.[3–7] Blind deconvolutions are less prevalent, although a sizable amount of research has been conducted recently.[8–13]

SeDDaRA is applicable when the degradation is space-invariant as it estimates the impulse function from the entirety of the data through power-law mapping. In cases where the degradation is not uniform across the data set, some restoration is still possible. However, this produces some non-physical artifacts. The algorithm has been applied successfully to images that contain significant noise. A formal study on the influence of noise has not yet been conducted.

2 Deconvolution Theory

The objective of data restoration is to remove degradation from data that, with an ideal detection system, would not be present. If the form of the degradation is known, a class of deconvolution processes can be used to remove the defect as best as possible. For one-dimensional signals, the degradation could be caused by unwanted low-pass filtering processes. For images, this degradation could be caused by motion blur, a partially blocked aperture, or an improperly focused lens system. The impulse function $d(x)$ represents how an impulse signal is received by the data collection system. A mathematical representation of the degraded data $g(x)$ is

$$g(x) = f(x) * d(x) + w(x) \tag{1}$$

where $f(x)$ is the truth data, $w(x)$ is a noise term, and $*$ denotes the convolution.[3] The objective is to find the best estimate of $f(x)$ from $g(x)$ when $d(x)$ and $w(x)$ are unknown. This relationship is simplified by transferring both sides of Equation 1 into frequency space via application of a Fourier transform,[14] yielding

$$G(u) = F(u)\ D(u) + W(u) \tag{2}$$

where u is the coordinate in frequency space, and the transformed functions are represented by capital letters.

If $d(x)$ is known, a deconvolution process can be applied to $g(x)$ to approximate $f(x)$. Many deconvolution algorithms, such as non-negative least squares and the Wiener filter, can be found in the literature.[3,15–17] For the following study, a pseudo-inverse filter will be used. The deconvolution is given by

$$F(u) = \frac{G(u)\ D^*(u)}{|D(u)|^2 + K} \tag{3}$$

where the parameter K is typically chosen by trial and error. This filter is easy to apply and works well with most data.

In many situations, $d(x)$ is not measurable and cannot be easily modelled. To address this, a range of solutions has been developed known as blind deconvolution algorithms. Blind deconvolution is a general term describing techniques that remove aberrations where $d(x)$ is unknown. Blind deconvolution techniques can be either iterative[8–12] or non-iterative .[13,18] Iterative techniques, which comprise of the majority of blind deconvolution techniques, are based on equations that require multiple applications. As such, they generally require a significant amount of computation and can be difficult to implement.[18] Often, both classes require that at least a certain amount of information about the degradation be known.

2.1 Derivation

The objective is to derive the transfer function $D(u)$ from $G(u)$ for use in a deconvolution algorithm. To do so, we assume the degradation is invariant, $D(u)$ is real, and has the form

$$D(u) = [K_G \mathcal{S}\{|G(u) - W(u)|\}]^{\alpha(u)} \tag{4}$$

where $\alpha(u)$ is a tuning parameter and K_G is a real, positive scalar chosen to ensure $|D(u)| \leq 1$. Application of the smoothing filter $\mathcal{S}\{...\}$ assumes that $D(u)$ is a slowly varying function. For images, a median filter consisting of a 3×3 pixel array is usually used.[3] Increasing the size of the array has the effect of reducing the influence of noise, but may limit the reconstruction of the higher frequency components.

Equation 4 is subject to the conditions that (i) $0 \leq \alpha(u) < 1$, (ii) the smoothing filter $\mathcal{S}\{...\}$ is separable, and (iii) that $F(u)$ and $W(u)$ are uncorrelated. Equation 4 states that application of a smoothing filter and power law to the power spectrum of the truth image, when chosen correctly, will produce the degradation. Although stated as an equality, in practice this is an approximation stemming from assumption (ii). For simplicity, $W(u)$ will be assumed negligible. To date, a formal study on the influence of significant noise has yet to be conducted.

Since $D(u)$ is assumed real, Equation 2 can be restated as

$$D(u) = \frac{\mathcal{S}\{|G(u)|\}}{\mathcal{S}\{|F(u)|\}} \tag{5}$$

where the smoothing operator has been applied. Since $D(u)$ is assumed to be a slowly varying function, it can be removed from the influence of the smoothing operator.

To solve for $\alpha(u)$, Equation 5 is substituted into Equation 4,

$$\frac{\mathcal{S}\{|G(u)|\}}{\mathcal{S}\{|F(u)|\}} \approx \frac{K_G \mathcal{S}\{|G(u)|\}}{K_{F'} \mathcal{S}\{|F'(u)|\}} \approx [K_G \mathcal{S}\{|G(u)|\}]^{\alpha(u)}. \tag{6}$$

Since the truth data $F(u)$ is unknown, we have replaced it with a data set $F'(u)$ that contains the desired characteristic frequency spectrum, where $K_{F'}$ is another scaling parameter. Given the presence of the smoothing filter, the replacement data set needs to satisfy

$$K_{F'} \mathcal{S}\{|F'(u)|\} \approx K_F \mathcal{S}\{|F(u)|\}. \tag{7}$$

Preferably, this function would be a theoretical model of the anticipated result with the source of the degradation removed from the equation. However, since modelling a detection system is often complicated, using an existing fair representation of the truth data can be more efficient. For example, an in-focus image of a terrestrial mountain can be used to restore an out-of-focus image of an extra-terrestrial landscape.

Solving for $\alpha(u)$ produces

$$\alpha(u) \approx \frac{\mathrm{Ln}[K_G \mathcal{S}|G(u)|] - \mathrm{Ln}[K_{F'} \mathcal{S}\{|F'(u)|\}]}{\mathrm{Ln}[K_G \mathcal{S}|G(u)|]}. \tag{8}$$

In this relation, K_G and $K_{F'}$ must be determined such that $|D(u)| \leq 1$. This condition is satisfied if we set $K_G = 1/\mathrm{Max}[\mathcal{S}\{|G(u)|\}]$ and $K_{F'} = 1/\mathrm{Max}[\mathcal{S}\{|F'(u)|\}]$.

It follows that

$$D(u) = \{K_G \mathcal{S}\{|G(u)|\}\}^{\alpha(u)} \tag{9}$$

where $\alpha(u)$ is given by Equation 8.

Substitution of Equation 8 into Equation 9 produces an approximation of Equation 5, providing a more concise result. Expressing the relation as a power law relation, however, enables one to approximate $\alpha(u)$ as a constant. This permits further simplification of the process, and comprises of a fully blind deconvolution algorithm. This approach is discussed in the next section.

2.2 Frequency-independent Alpha

In some situations, the function $\alpha(u)$ can be approximated by a constant value. For example, most natural scenes possess a frequency spectrum that peaks in the lowest frequency range, and rapidly decreases for higher spatial frequencies. Application of a power law, i.e. using a constant value for α with $0 \leq \alpha < 1$, can enhance the part of the curve that is most affected by a blur function.

This is demonstrated by the following images. Figure 1 is an image of a bowl of fruit (top) and its convolution (bottom) with a point spread function. The frequency-dependent deconvolution algorithm was applied to the image to produce $\alpha(u)$. A line plot of the function is shown in Figure 2. Aside from the lowest frequencies, $\alpha(u)$ can be approximated as $\alpha = 0.28$. Using this value and the frequency independent method, a point spread function was extracted and used to deconvolve the image. The result, shown in Figure 3, (top) is a significant improvement over Figure 1 (bottom), and compares favorably to either the truth image or the frequency-dependent deconvolution, shown in Figure 3 (bottom). The function $|F(u)'|$ in this case has been derived from the actual truth image.

The value α becomes a tuning parameter satisfying $0 \leq \alpha < 1$, chosen by trial and error. In most cases, $\alpha = 0.5$ has proven to be an effective initial choice. Reconstruction quality does not significantly differ for variations less than ± 0.05. This approach has been discussed in a previous paper.[1]

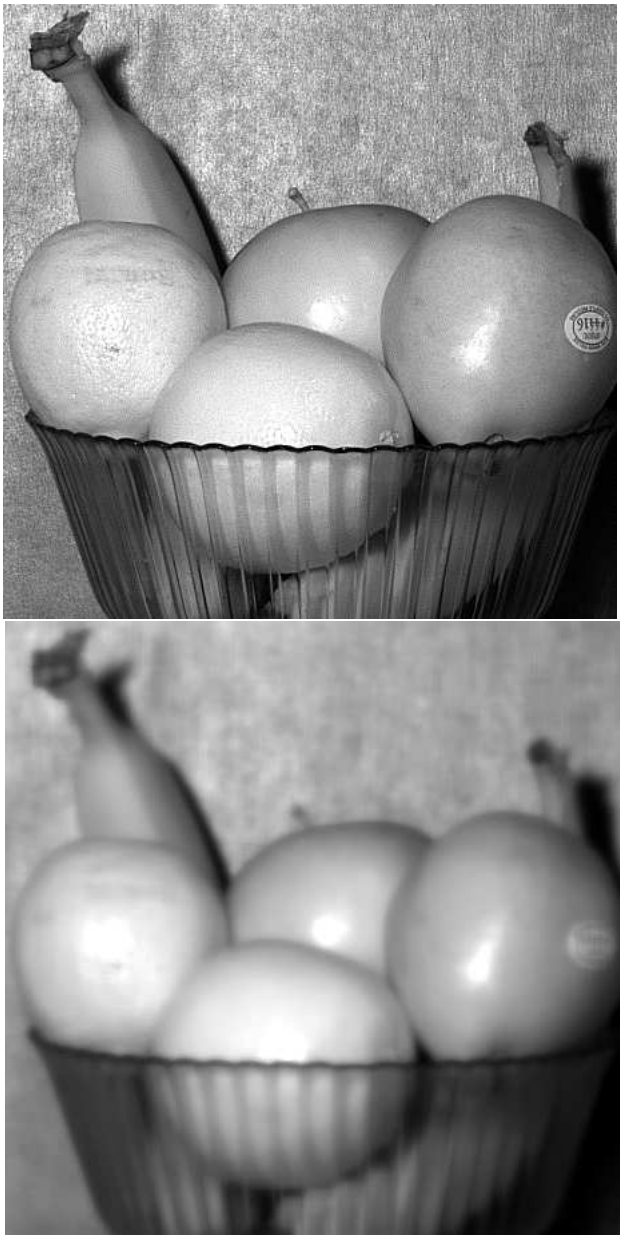

Figure 1: Top: Truth image of a bowl of fruit taken with a digital camera. Bottom: The convolution of the image with a point spread function.

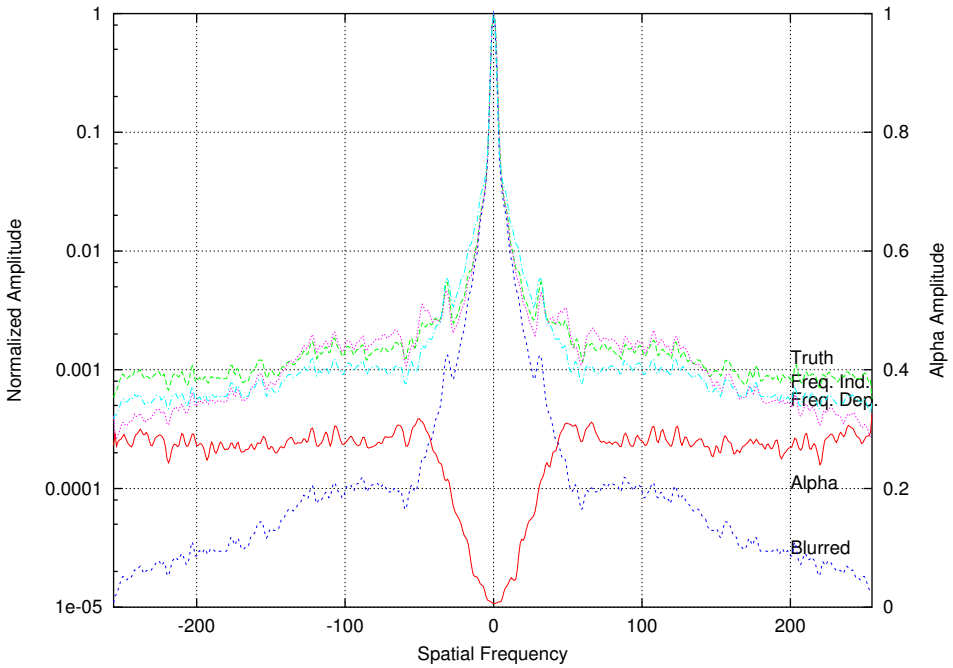

Figure 2: A line plot of the frequency spectrum of the four images. The y-axis is a logarithmic plot of the frequency response amplitude normalized to unity. The second y-axis is a plot of the alpha function. Notice how the value can be approximated by 0.28 for all but the lowest frequencies.

3 Examples

This technique has been applied to an image of the surface of the moon Io of Jupiter taken by the space probe Galileo,[19] shown in Figure 4 (top). Although the image exhibits good resolution, the application of SeDDaRA, shown in Figure 4 (bottom), brings out more detail. This resolution used a synthetic Mandelbrot-type fractal image as the source for $|F(u)'|$.

The detail in Figure 4 (top) may be recovered by standard means, such as applying an edge filter. However, edge filters can only be described as an image enhancement technique, amplifying spatial frequencies to improve the image visually. SeDDaRA, however, is a true image restoration technique, restoring frequencies that were degraded by system optics and electronics. There is less danger of introducing features not present in the original image.

As an example of application on non-optical imagery, Figure 5 is an x-ray image of a muscovy duck.[20] The restoration displays features that were not visually perceptible in the original image. The source for the representative truth image, $|F(u)'|$, was Figure 1 (top). A line plot was made across one wing to demonstrate the improvement in contrast and resolution. This is shown in Figure 6.

Figure 7 (top) displays a original and restored ultrasound waveform that has travelled through air for about a centimeter.[21] In this frequency range, higher frequencies are greatly attenuated. Using Equation 9 and a reference waveform, the frequency-

Figure 3: Top: Restoration of the image using $\alpha = 0.28$ and a pseudo-inverse filter. Bottom: Restoration of the image using a frequency-dependent $\alpha(u)$ and a pseudo-inverse filter.

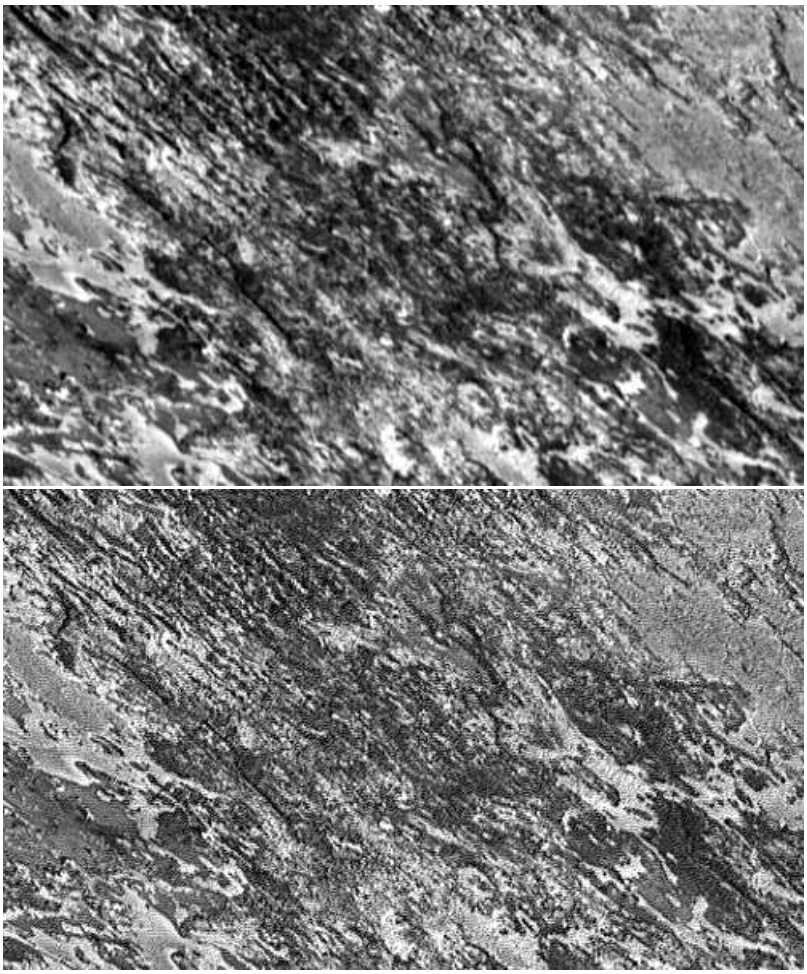

Figure 4: This image (top) was taken by the space probe Galileo of the surface of Io.[19] Although the image already exhibits a fair amount of high resolution, application of the frequency-dependent restoration process brings out more detail (bottom).

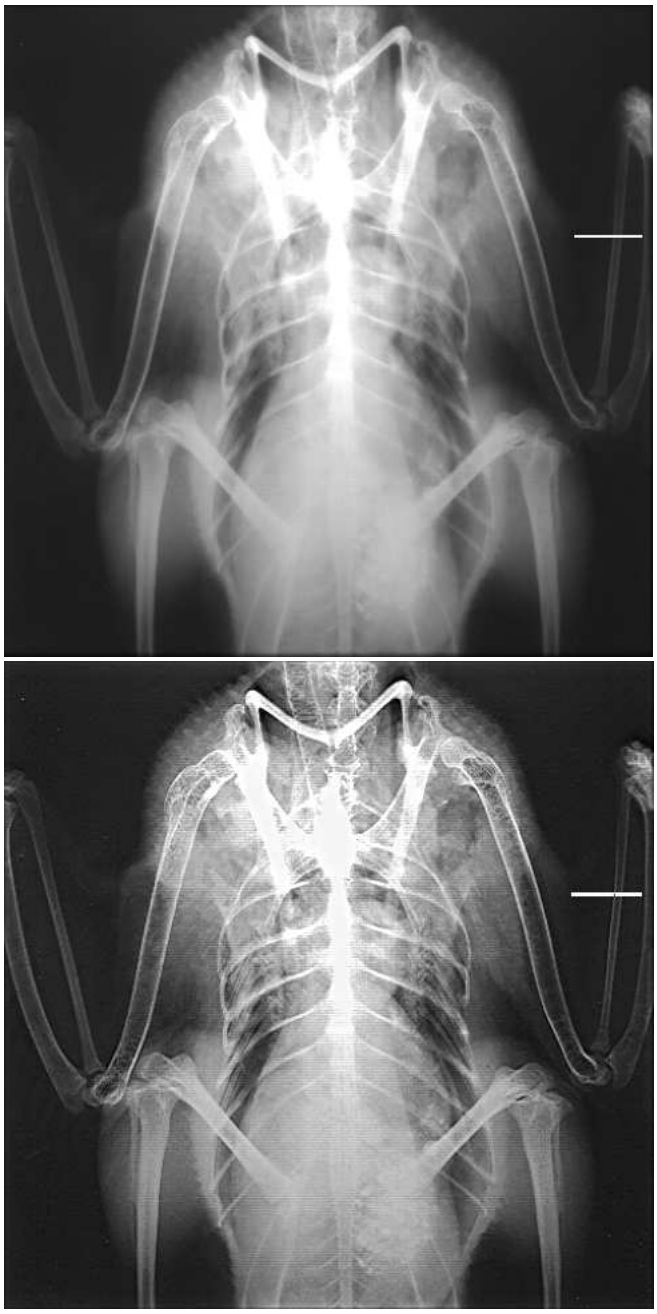

Figure 5: This image (top) is an x-ray of a muscovy duck.[20] The deconvolution (bottom) was restored with a frequency-dependent $\alpha(u)$. The white line indicates the path of the line plot shown in Figure 6.

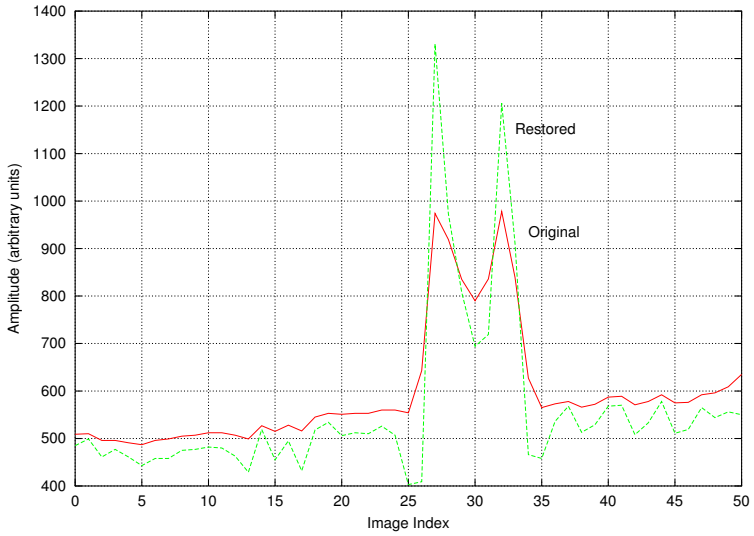

Figure 6: This is a line plot taken across the wing as shown in Figure 5. The restored image shows improved resolution when the algorithm is applied.

dependent $\alpha(u)$ was extracted from the image. The transfer function was created and inserted into the deconvolution algorithm. The source for the representative truth data was a synthetic waveform. The restored waveform exhibits additional peaks and features that had not been apparent before. The frequency spectra are shown in Figure 7 (bottom).

As shown in the examples, the high frequency content is significantly enhanced through this process. However, with any blind deconvolution technique, there is a risk of introducing non-physical artifacts, such as the deep valley at image index 25 in Figure 6, most likely the result of the influence of the pseudo-inverse filter. Although new features, such as those in Figure 7 (top), can be revealed using this technique, their physical existence should be verified independently if possible.

4 Conclusion

The SeDDaRA process has several unique characteristics that are not found in current signal processing algorithms. At the core of the process, the application of this method extracts a reasonably good approximation for the degradation of a signal in a comparatively short amount of time, provided the degradation is invariant across the data set. This algorithm is easy to implement, and can be inserted into existing signal processing packages without much difficulty. As demonstrated, the method works well on a wide variety of signal types, including imagery, acoustic waveforms, and any signal that suffers from low-pass filtering. This is accomplished without direct information about the type or extent of aberration.

Potential commercial applications include image processing, for both research-based and consumer-based imagery. Aging photographs and movies may be restored and preserved digitally, or reprinted. Non-optical images such as medical ultrasound

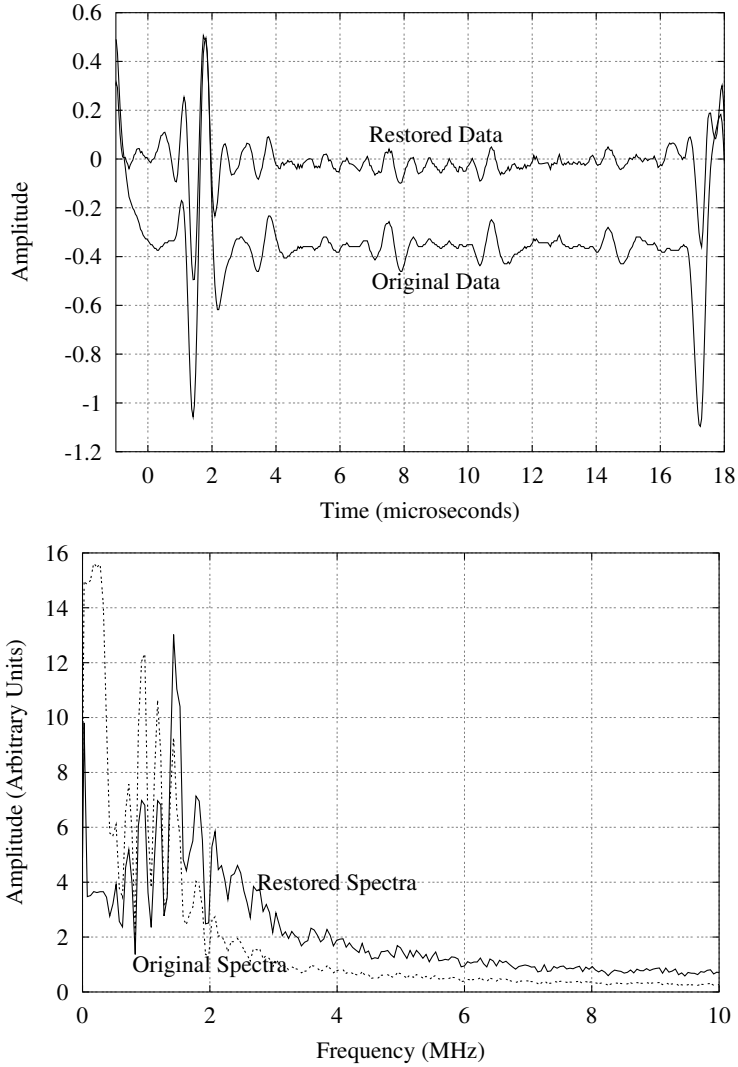

Figure 7: (Top) The lower plot (labelled 'Original Data') is an ultrasound waveform that travelled through a centimeter of air. In this frequency range, the higher frequencies are strongly attenuated by air.[21] The frequency-dependent alpha function was determined using Equation 9, producing an appropriate transfer function. The data was deconvolved using the extracted filter function. The restored data (labelled 'Restored Data') exhibits several peaks that were not apparent in the original data. An arbitrary offset was added to the data for demonstrative purposes. The frequency spectra are shown on the bottom graph. Note the improved higher frequency sensitivity between 1 and 4 MHz.

scans and X-rays scan can also be improved. This technique can be a valuable research tool to recover the full bandwidth of a signal, restoring the high-frequency content. SeDDaRA may find application in recording studios and home sound systems to counteract effects created by room acoustics, and enhance the quality of the reproduction.

References

[1] J.N. Caron, N.M. Namazi, R.L. Lucke, C.J. Rollins, and P.R. Lynn, Jr., "Blind data restoration with an extracted filter function," *Optics Letters* **26(15)**, 1164–1166, 2001.

[2] J.N. Caron, U.S. Patent pending, anticipated acceptance date: August, 2003.

[3] A.K. Jain,"Fundamentals of digital image processing," Prentice-Hall, Englewood Cliffs, NJ 07632, 1989.

[4] M.I. Sezan, "Survey of recent developments in digital image restoration," Optical Engineering, **29(5)**, 393–404 (1990).

[5] B. Jähne, "Digital Image Processing," Springer-Verlag, Berlin, Germany, 1997.

[6] P.M. Clarkson and H. Stark, eds., "Signal processing methods for audio, images, and telecommunications," Academic Press, San Diego, CA, 1995.

[7] J.G. Proakis and D.G. Manolakis, "Introduction to signal processing," Macmillan Publishing Company, New York, NY, 1988.

[8] N.F. Law and D.T. Nguyen, "Multiple frame projection based blind deconvolution," Electronics Letters **31(20)**, 1733–1734 (1995).

[9] S. Barraza-Felix and B.R. Frieden, "Regularization of the image division approach to blind deconvolution," Applied Optics **38(11)**, 2232–2239 (1999).

[10] O. Shalvi and E. Weinstein, "Super-exponential methods for blind deconvolution," IEEE Transactions on Information Theory **39(2)**, 504–519 (1993).

[11] B.L. Satherly, and P.J. Bones, "Zero tracks for blind deconvolution of blurred ensembles," Applied Optics **33(11)**, 2197–2205 (1994).

[12] Ayers, and Dainty, "Iterative Blind Deconvolution Method and Its Applications," Optics Letters, **13**, 547–549 (1988).

[13] Y. Yitzhaky, R. Milberg, S. Yohaev, and N.S. Kopeika "Comparison of direct blind deconvolution methods for motion-blurred images," Applied Optics **38(20)**, 4325–4332 (1999).

[14] G. Arfken, "Mathematical Methods for Physicists", Academic Press, San Diego, CA 92101, 1985.

[15] N. Wiener, "The Extrapolation, Interpolation, and Smoothing of Stationary Time Series with Engineering Applications," Wiley, New York, 1949.

[16] C.W. Helstrom, "Image restoration by the method of least-squares," Journal of the Optical Society of America **57**, 297–303 (1967).

[17] D. Slepian, "Linear least-squares filtering of distorted images," Journal of the Optical Society of America **57**, 918–922 (1998).

[18] Y. Yitzhaky, I. Mor, A. Lantzman, and N.S. Kopeika "Direct method for restoration of motion-blurred images," Journal of the Optical Society of America A **15(6)**, 1512–1519 (1998).

[19] Image courtesy of NASA/JPL/Caltech.

[20] Image courtesy of the Arizona Board of Regents and the Center for Image Processing in Education, Tuscon, AZ.

[21] J.N. Caron, Y. Yang, J.B. Mehl, and K.V. Steiner, "Gas-coupled laser acoustic detection for ultrasound inspection of composite materials," *Materials Evaluation*, **58(5)**, 667–671, 2000.